



Published in final edited form as:

Bioconjug Chem. 2008 September ; 19(9): 1803–1812. doi:10.1021/bc8001375.

Evaluation of the Pharmacokinetic Effects of Various Linking Group Using the ^{111}In -DOTA-X-BBN(7-14) NH_2 Structural Paradigm in a Prostate Cancer Model

Jered C. Garrison[†], Tammy L. Rold[†], Gary L. Sieckman[‡], Farah Naz[†], Samantha Sublett[‡], Said Daibes Figueroa^{‡,§}, Wynn A. Volkert[§], and Timothy J. Hoffman^{*,†,‡,∞}

[†]Department of Internal Medicine, MA408 Medical Science Building, University of Missouri-Columbia School of Medicine, Columbia, MO 65212

[‡]Research Services, Harry S Truman Memorial Veterans' Hospital, 800 Hospital Dr., Columbia, MO 65201

[§]Department of Radiology, One Hospital Dr., University of Missouri-Columbia School of Medicine, Columbia, MO 65212

[∞]Department of Chemistry, University of Missouri-Columbia, 601 S. College Avenue, Columbia, MO 65211

Abstract

The high incidence of BB2 receptor (BB2r) expression in various cancers has prompted investigators to pursue the development of BB2r-targeted agents for diagnostic imaging, chemotherapy and radiotherapy. Development of BB2r-targeted agents, based on the bombesin (BBN) peptide, has largely involved the use of the bifunctional chelate approach in which the linking group serves several key roles including pharmacokinetic modification. Understanding the *in vivo* properties of the various pharmacokinetic modifying linking groups is crucial for developing BB2r-targeted agents with improved targeting and clearance characteristics. The goal of this study was to systematically evaluate the pharmacokinetic profile of aliphatic hydrocarbon, aromatic and polyethylene glycol (ether) functional groups in order to obtain a better understanding of the *in vivo* properties of these pharmacokinetic modifiers. Specifically, we synthesized six radioconjugates with the structure ^{111}In -DOTA-X-BBN(7-14) NH_2 , where X = 8-aminooctanoic acid (8-AOC), 5-amino-3-oxapentyl-succinamic acid (5-ADS), 8-amino-3,6-dioxaoctyl-succinamic acid (8-AOS), *p*-aminobenzoic acid (AMBA), Gly-AMBA and Gly-*p*-aminomethylbenzoic acid (Gly-AM2BA). All of the ^{111}In -conjugates demonstrated nanomolar binding affinities to the BB2r. In CF-1 mice, the BB2r uptake in the pancreas of radioconjugates containing aromatic linking groups was found to be significantly higher at 1 hr post-injection than the radioconjugates with ether linker moieties. For PC-3 tumor bearing SCID mice, the tumor uptake was found to be 6.66 ± 2.00 , 6.21 ± 1.57 , 6.36 ± 1.60 , 4.46 ± 0.81 and 7.76 ± 1.19 %ID/g for the 8-AOC, 8-ADS, AMBA, Gly-AMBA and Gly-AM2BA radioconjugates, respectively, at 15 min post-injection. By 24 hr post-injection, the radioconjugates containing aromatic groups exhibited the highest percentage tumor retention with 11.4, 19.8, 26.6, 25.8 and 25.5% relative to the 15 min values remaining in the tumor tissue for the 8-AOC, 8-ADS, AMBA, Gly-AMBA and Gly-AM2BA radioconjugates, respectively. Fused Micro-

*To whom correspondence should be addressed. Telephone: (573) 814-6000 Ext. 52593. Fax: (573) 882-1663. E-mail: HoffmanT@health.missouri.edu.

[†]Abbreviations used: BB1r, Neuromedin B receptor; BB2r, Gastrin-releasing peptide receptor; BB3r, orphan receptor; BB4r, Bombesin receptor; DOTA, 1,4,7,10-tetraazacyclododecane-N,N',N'',N'''-tetraacetic acid, BBN, Bombesin peptide; SPECT, Single photon emission computed tomography; PET, Positron emission tomography; 8-AOC, 8-aminooctanoic acid; 5-ADS, 5-amino-3-oxapentyl-succinamic acid; 8-AOS, 8-amino-3,6-dioxaoctyl-succinamic acid; AMBA, *p*-aminobenzoic acid; Gly-AMBA, Glycine-*p*-aminobenzoic acid; Gly-AM2BA, Glycine-*p*-aminomethylbenzoic acid; NONSENSE, H-M-G-W-L-A-Q-V-NH₂.

SPECT/CT imaging studies performed at 24 hr post-injection revealed substantial accumulation of radioactivity in the tumor tissue for all radioconjugates. In both biodistribution and Micro-SPECT/CT imaging studies, the radioconjugates containing aromatic linking groups typically exhibited significantly higher G.I. tract retention than the hydrocarbon or ether linking moieties. In conclusion, our studies indicate that radioconjugates incorporating aromatic linking groups, of the type investigated, generally demonstrated enhanced retention in BB2r expressing tissues in comparison to either the hydrocarbon or ether linking moieties. Furthermore, this investigation clearly demonstrates the significance of the linking group upon not only the *in vivo* clearance of the radiopharmaceutical, but on the *in vivo* uptake and retention of the BB2r-targeted agent in tumor tissue. Future designs of BB2r-targeted agents should include a careful consideration of the effect linking group functionality has upon tumor targeting and retention.

Introduction

The bombesin family of receptors currently consists of four known receptor subtypes: BB1r, neuromedin B receptor; BB2r, gastrin-releasing peptide receptor; BB3r, orphan receptor and BB4r, bombesin receptor.(1,2) Of these four receptors, three (BB1r, BB2r and BB3r) have been shown to be expressed in varying degrees in a variety of human tumors and human cancer cell lines.(3,4) For prostate and breast carcinomas, the BB2r subtype has received the most attention from the research community due to the high expression density of the receptor relative to the BB1r and BB3r subtypes.(4-6) In normal human tissues, the pancreas has been shown to have the highest degree of BB2r gene expression with significantly lower levels in the stomach, brain and adrenal glands.(7) The low expression of the BB2r in normal tissue relative to the increased expression in many cancers has validated the BB2r as a target for cancer detection and treatment. This has prompted the development of a wide variety of BB2r-targeted diagnostic imaging, chemotherapy and radiotherapy agents. The majority of these agents have been based on bombesin, a 14 amino acid peptide. The BB2r binding region of the bombesin (BBN) peptide (Trp-Ala-Val-Gly-His-Leu-Met-NH₂, BBN(8-14)NH₂) shares a sequence homology with the Gastrin-Releasing Peptide, the native ligand to the BB2r. Upon binding of the agonist bombesin analog to the BB2r, the peptide and the attached chemotherapy agent and/or radionuclide is internalized and thereby retained in the cell.

The bifunctional chelate design has primarily been used in the development of BB2r-targeted BBN analogs for nuclear diagnostic imaging and radiotherapy. This approach has four distinctive components: a targeting vector, radiometal, chelation system and linking group. The choice of targeting vectors for the bombesin analogs have varied from the use of the entire 14 amino acid bombesin peptide to truncated portions of the peptide, with the latter being most prevalent in the literature. In any event, the targeting vector must employ the BBN(8-14)NH₂ or a BB2r-targeted derivative of this amino acid sequence in order to achieve uptake in BB2r expressing tissues. To date, a wide variety of radionuclides (e.g. ^{99m}Tc, ¹⁸⁸Re, ⁹⁰Y, ¹¹¹In, ¹⁸F, ⁶⁴Cu, ¹⁷⁷Lu, ¹⁴⁹Pm, ⁶⁸Ga) have been used in the development of BB2-targeting peptides.(8-16) The selection of the radionuclide for the BB2r-targeted BBN analog is largely influenced by the desired function of the radiopharmaceutical. Diagnostic nuclear imaging agents employ radionuclides with gamma and positron emission properties that are appropriate for Single Photon Emission Computed Tomography (SPECT) or Positron Emission Tomography (PET), respectively. For targeted radiotherapy, radionuclides are selected to deliver a maximum radiation dose to the cancerous tissue based on tumor residence time, while, at the same time, attempting to ensure minimal damage to non-target tissues.(17) The chelation system, in general, is responsible for the binding of the radiometal and preventing transchelation throughout the *in vivo* lifetime of the radiopharmaceutical. The selection of the chelation system is largely dependent on the chemical nature of the radionuclide; however, an assortment of chelation systems (e.g. DOTA,

TETA, DTPA) have been shown to be effective in stabilizing a variety of radionuclides in vivo. (8,18-20)

The linking group serves several crucial roles in the bifunctional chelate design of BB2r-targeted BBN analogs. The most obvious role of the linking group is to chemically connect the radiometal-chelation complex to the bombesin targeting vector. The linking group is also responsible for preventing the radiometal-chelation complex from interfering with the binding of the bombesin targeting vector to the BB2r. Our laboratory has demonstrated, using hydrocarbon based linking groups, that the length of the linking group being employed directly impacts in vitro and in vivo BB2r targeting.(9) These studies demonstrated that a linker length of > 6 carbon atoms long, which corresponds to ~ 6.5 Å, is needed to ensure optimal in vivo binding of the bombesin targeting vector to the BB2r. Lastly, the linking group serves as a convenient chemical handle in which to modify the pharmacokinetics of the radiopharmaceutical. By altering the hydrophilic or hydrophobic properties of the linking group, the in vivo properties of the BB2r-targeted BBN analog can often be tailored without altering the structure of the targeting vector and/or the radiometal-chelation complex thereby avoiding changes that may have negative impacts on in vivo BB2r binding and/or radiometal-chelate stability.

Targeted diagnostic and radiotherapy agents based on small peptides and antibodies have employed an assortment of natural and non-natural cationic, anionic, and neutral amino acids in constructing the linker framework.(19) Additionally, metabolically active linking groups based on esters, disulfides, protease active amino acid sequences and other cleavable functional groups have been explored.(21,22) For BB2r-targeted BBN based radiopharmaceuticals, a variety of aliphatic hydrocarbons, amino acids, aromatic derivatives and polyethylene glycol units have been utilized in the design of linking groups.(1,2,14,23-25) The in vivo effect of these different functional linking groups is challenging to assess due to difficulty in comparing BB2r-targeted BBN analogs that employ different components (i.e. targeting vectors, radionuclides and chelation systems). In order to systematically determine the pharmacokinetic profile of some commonly used functional groups, we decided to synthesize and evaluate BB2r-targeted BBN analogs containing an aliphatic hydrocarbon, aromatic derivatives and polyethylene glycol derivatives. Specifically, six radioconjugates were synthesized and evaluated using the $^{111}\text{In-DOTA-X-BBN}(7-14)\text{NH}_2$ structural paradigm where **X** = 8-aminooctanoic acid (8-AOC), 5-amino-3-oxapentyl-succinamic acid (5-ADS), 8-amino-3,6-dioxaoctyl-succinamic acid (8-AOS), *p*-aminobenzoic acid (AMBA), Gly-AMBA and Gly-*p*-aminomethylbenzoic acid (Gly-AM2BA). The synthesis, in vitro and in vivo evaluation of the radioconjugates in a PC-3 prostate cancer model is presented below.

Materials and Methods

Unless otherwise noted, all chemicals and reagents were used as received. Indium-111 was purchased from Mallinckrodt (Maryland Heights, MO, U.S.A.). Fmoc-protected natural amino acids, Fmoc-*p*-aminobenzoic acid, Fmoc-*p*-aminomethylbenzoic acid and Rink Amide resins were purchased from EMD Biosciences Inc. (San Diego, CA, U.S.A.). Tris(1,1-dimethylethyl)-1,4,7,10-tetraazacyclododecane-1,4,7,10-tetraacetic acid was purchased from Macrocyclics (Dallas, TX, U.S.A.). N-(Fmoc-5-amino-3-oxapentyl)-succinamic acid and N-(Fmoc-8-amino-3,6-dioxaoctyl)-succinamic acid were purchased from NeoMPS (San Diego, CA, U.S.A.). Fmoc-8-Aminooctanoic acid was purchased from Advanced ChemTech (Louisville, KY, U.S.A.). Naturally abundant indium chloride was purchased from Strem Chemicals Inc. (Newburyport, MA, U.S.A.). HPLC grade acetonitrile and trifluoroacetic acid were purchased from Fischer Scientific (Pittsburg, PA, U.S.A.). Deionized water used for HPLC analyses and all other chemical applications in this work was obtained from an in-house Millipore (Billerica, MA, U.S.A.) Milli-Q Biocel water purification system. Roswell Park

Memorial Institute (RPMI) 1640 media was purchased from Invitrogen/GIBCO (Carlsbad, CA, U.S.A.). 4-(2-hydroxyethyl)-1-piperazineethanesulfonic acid (HEPES) and bovine serum albumin (BSA) was purchased from Fisher Scientific (Fisher Bioreagents, Fisher Chemical, Fairlawn, NJ, U.S.A.). [¹²⁵I-Tyr⁴]BN (10 μCi, 370 kBq) was purchased from Perkin Elmer (Wellesley, MA, U.S.A.). Isoflurane was purchased from Baxter Healthcare Corp. (Deerfield, IL, U.S.A.).

Solid Phase Peptide Synthesis (SPPS) was performed using an Applied Biosystems (Foster City, CA, U.S.A.) Model 432 automated peptide synthesizer using standard Fmoc chemistry. RP-HPLC purification of the conjugates, ^{nat}In-conjugates and ¹¹¹In-radioconjugates was accomplished using a Waters (Milford, MA, U.S.A.) 600E controller equipped with an Eppendorf (Westbury, NY, U.S.A.) TC-50 column heater. A Phenomenex (Torrance, CA, U.S.A.) Jupiter 5u C₁₈ 300 Å 250 × 10 mm semi-prep column was used for the purification of bulk amounts of peptides. For the purification of conjugates, ^{nat}In-conjugates and ¹¹¹In-radioconjugates used for mass spectrometric, in vitro and in vivo studies a Phenomenex Jupiter 5u C₁₈ 300 Å 250 × 4.60 mm analytical column was employed. Detection of the conjugates and ^{nat}In-conjugates during HPLC purification was accomplished using a JASCO (Easton, MD) UV 975 absorbance detector. The radioconjugates were detected during HPLC purification using a JASCO UV 1575 absorbance detector and an ORTEC (Oak Ridge, TN, U.S.A.) NaI(Tl) scintillation detector. During the preparation of the radioconjugates, 3M (St. Paul, MN, U.S.A.) Empore High Performance Extraction Disk Cartridges 4215(HD) were employed. Mass spectrometric determination of the conjugates and ^{nat}In-conjugates was achieved using electrospray ionization with a Thermo-Finnigan TSQ7000 triple-quadrupole mass spectrometer equipped with an API2 source and Performance Pack. Gamma decay detection of ¹¹¹In for the in vitro binding studies was accomplished using the Packard Riastar (Downers Grove, IL, U.S.A.) gamma counter. Pharmacokinetic gamma decay measurements were made using a well counter equipped with a NaI(Tl) scintillation detector.

Carworth Farms No. 1 (CF-1) mice were purchased from Charles Rivers Laboratories (Wilmington, MA). Four to five week-old Institute of Cancer Research Severely Combined Immunodeficient (ICR SCID) mice were obtained from Taconic Farms (Germantown, NY, U.S.A.). The mice were supplied with acidified water and irradiated rodent chow (Ralston Purina Co.) ad libitum. Five mice were housed per cage (Alternative Design) in a humidity- and temperature-controlled room with a 12 hour light/dark cycle. The human prostate cancer PC-3 cell line was purchased from the American Type Culture Collection (ATCC, Rockville, MD). The PC-3 cell line was grown and maintained by the University of Missouri Cell and Immunobiology Core Facility. PC-3 cells were grown in Custom RPMI Medium 1640 supplemented with 10% Fetal Bovine Serum (FBS), (U.S. Bio-Technologies Inc., Pottstown, PA) and Gentamicin (American Pharmaceutical Partners, Inc., Schaumburg, IL). To prepare the cells for inoculation, the PC-3 cells with media were centrifuged, the media decanted, and the cell pellet combined with Dulbecco's phosphate-buffered saline (Invitrogen Corporation, Carlsbad, CA) to reach a concentration of 5 million cells/100μL. Under gas anesthesia, each SCID mouse was subcutaneously inoculated (bilateral flank) with 5 million PC-3 tumor cells in each flank. Using a non-rebreathing apparatus (Summit Medical Equipment Company, Bend, OR), gas anesthesia was administered at a vaporizer setting of ~3.5% isoflurane (Baxter Healthcare Corp., Deerfield, IL) with ~1 L/min oxygen. The flank tumors were allowed to grow for 2 - 3 weeks before studies were performed. All studies involving animals were conducted in accordance with protocols approved by both the Harry S Truman Veterans' Hospital and the University of Missouri – Columbia Institutional Animal Care and Use Committees.

Solid Phase Peptide Synthesis (SPPS)

The conjugates were assembled using automated peptide synthesis. Briefly, the resin (25 μ mole of the resin substituted peptide anchors) was deprotected using piperidine resulting in the formation of a primary amine from which the C-terminus of the growing peptide was anchored. The Fmoc protected amino acids (75 μ mole) with appropriate orthogonal protection were activated using HBTU and sequentially added to the resin. The resulting peptide was orthogonally deprotected and cleaved from the resin using a cocktail consisting of a 2:1:1:36 ratio of thioanisole, water, 1,2-ethanedithiol and trifluoroacetic acid, respectively. The cleaved peptide was then precipitated and washed using cold (0°C) methyl-*tert*-butylether. The crude conjugate was dried by vacuum, weighed and analyzed by RP-HPLC. Purity of the crude peptides, as determined by RP-HPLC, varied depending on the peptide. The DOTA-8-AOC-BBN(7-14)NH₂, DOTA-8-AOC-NONSENSE, DOTA-5-AOS-BBN(7-14)NH₂ and DOTA-8-ADS-BBN(7-14)NH₂ conjugates ranged from 55 - 76% pure by RP-HPLC. The DOTA-Gly-AM2BA-BBN(7-14)NH₂ conjugate was synthesized in a modest 47% yield. The DOTA-AMBA-BBN(7-14)NH₂ and DOTA-Gly-AMBA-BBN(7-14)NH₂ conjugates yielded crude products that were found to be 21 and 12%, respectively, by RP-HPLC. For the DOTA-AMBA-BBN(7-14)NH₂, DOTA-Gly-AMBA-BBN(7-14)NH₂ and DOTA-Gly-AM2BA-BBN(7-14)NH₂ conjugates, these peptides were purified using semi-preparative RP-HPLC before studies were performed. All conjugates were peak purified to $\geq 93\%$ purity and quantified by analytical RP-HPLC prior to mass spectrometric determination and in vitro cell binding assays. Confirmation of the constitution of the desired conjugates was provided by mass spectrometry.

Syntheses of ^{nat}In conjugates

A 1 mg sample of the conjugate was dissolved in 500 μ L of a 0.1 M ammonium acetate, 1.82 mM indium trichloride solution (pH = 5.5). The solution was heated at 60°C for 30 minutes. In order to achieve sufficient separation (~ 2 min) of the ¹¹¹In-labeled conjugate from the unlabeled conjugate, solid ^{nat}CuSO₄•5H₂O was added to the solution. The solution was heated for 5 min at 65°C and allowed to cool to room temperature. ^{nat}In-conjugates were then peak purified and quantified by RP-HPLC. All ^{nat}In-conjugates were determined to be $\geq 93\%$ pure by RP-HPLC analyses before mass spectrometric characterization and in vitro binding studies were performed.

Radiolabeling of conjugates with ¹¹¹InCl₃

A 100 μ g sample of the conjugate and ~20 mg of L-Ascorbic Acid (radiolysis prevention reagent) was dissolved in 200 μ L of a 0.4 M ammonium acetate (pH = 7.0) solution. An aliquot of ¹¹¹InCl₃ (18.5 – 92.5 MBq) was added to the vial containing the conjugate and the solution was heated for 30 - 40 min at 65 - 75°C. In order to achieve adequate peak separation (~ 2 min), solid ^{nat}CuSO₄•5H₂O was added to the solution. The solution was heated for 5 min at 65°C and allowed to cool to room temperature. The resulting ¹¹¹In-radioconjugate was peak purified using reverse phase HPLC. The peak purified ¹¹¹In-radioconjugate was concentrated using a prepared C₁₈ extraction disk and eluted with 400 μ L of a 6:4 ethanol:sterile saline solution. For pharmacokinetic studies, the purified ¹¹¹In-radioconjugates were diluted with sterile saline to 185 kBq/100 μ L. The purification of the radioconjugate and the use of carrier-free ¹¹¹In yielded the purified ¹¹¹In-radioconjugates with a specific activity in the order of the theoretical maximum (Theo. Max: 1722 GBq/ μ mol). Pre-clinical SPECT imaging studies required 27.8 – 55.5 MBq/mouse necessitating the evaporation of the ethanol from the ethanolic ¹¹¹In-radioconjugate solution under a stream of nitrogen and dilution to the appropriate volume with sterile saline solution. In all cases, the concentration of ethanol in solution was < 8% by volume prior to administration. Overall radiochemical yields typically ranged from 35 - 89%. The radiochemical purity of all ¹¹¹In-radioconjugates for pharmacokinetic and imaging studies were reassessed prior to administration and found to be $\geq 93\%$ pure.

HPLC purification and analyses

When necessary, bulk sample purification was performed using a semi-preparative C₁₈ column with a flow rate of 5.0 mL/min. Sample purification for mass spectrometric, in vitro and in vivo studies was performed on an analytical C₁₈ column with a flow rate of 1.5 mL/min. For all HPLC experiments, the mobile phase consisted of solvent A (99.9% H₂O and 0.1% TFA) and solvent B (99.9% CH₃CN and 0.1% TFA). For all conjugates, ^{nat}In-conjugates and ¹¹¹In-radioconjugates, the gradient was initiated at 80% A: 20% B and over a period of 15 minutes linearly decreased to a gradient of 70% A: 30% B. At the end of the 15 minute run time for all HPLC experiments, the column was flushed with the gradient 5% A: 95% B and re-equilibrated at the starting gradient.

In Vitro Competitive Cell Binding Studies

IC₅₀ binding studies for all conjugates and ^{nat}In-conjugates were performed using PC-3 human prostate cancer cells. ^{nat}In-conjugates were used to determine the specific binding affinities for the corresponding ¹¹¹In-radioconjugates. Cell media consisted of Roswell Park Memorial Institute (RPMI) medium at pH 7.4, 4.8 mg/mL HEPES and 2 mg/mL BSA. For binding assays, the cells (~3×10⁴ PC-3 cells) were suspended in media and incubated at 37°C for 40 min in the presence of radiolabeled [¹²⁵I-Tyr⁴]BN, a known BB2r agonist, and a range of molar concentrations (10⁻⁶ - 10⁻¹² M) of the conjugate or ^{nat}In-conjugate. At the end of the incubation period, the cells were aspirated and washed 4 X with media. The cell associated activity was measured and the binding affinity determined.

In Vitro Internalization and Efflux Assays

Internalization and efflux studies were performed by incubating 3 × 10⁴ PC-3 human cancer cells in cell media. The cell media consisted of RPMI medium with 2 mg/mL BSA and 2.8 mg/mL HEPES at a pH of 7.4. For the internalization studies, the cells were incubated at 37°C with 20,000 cpm of the desired ¹¹¹In-radioconjugate in the presence of 5% CO₂ for 15, 30, 45, 60, 90 and 120 min time points. At the end of the time point, binding was halted by aspiration of the cell medium and washing of the cells (3X) with ice cold cell culture medium. Surface bound radioactivity was removed from the cellular membrane surface by addition of ice cold pH 2.5 saline buffer (0.2 M acetic acid and 0.5 M NaCl). The cells were vortexed and incubated in the medium for 5 min, followed by the removal of the radioactivity in the supernatant by aspiration and washing the cells (2X) with pH 2.5 saline buffer. The radioactivity as a function of time was determined for the supernatant and the cells, which yielded the percent radioactivity surface bound and internalized, respectively.

Efflux assays were performed by incubating the PC-3 cells with the desired ¹¹¹In-radioconjugate for 45 minutes. After this time, the cellular medium was aspirated and washed with 37°C cell medium (3X). At 15, 30, 45, 60 and 90 min time points post-incubation, samples of the incubated cellular medium were collected and the cellular media was aspirated and washed with ice cold culture medium. This was followed by aspiration and washing of the cells with ice cold pH 2.5 saline buffer. The radioactivity as a function of time was determined for the supernatant and the cells which yielded the percent radioactivity effluxed from the cell and the percent remaining internalized, respectively.

Pharmacokinetic Studies of ¹¹¹In-radioconjugates in normal CF-1 and PC-3 xenograft SCID mice

Pharmacokinetic studies were carried out using age matched normal CF-1 and PC-3 tumor bearing SCID mice. For pharmacokinetic studies involving PC-3 xenograft SCID mice, the mice were inoculated with PC-3 cells and the tumors, ranging from 0.1 to 1.0 g (2-3 weeks post inoculation), were allowed to develop before the mice were utilized in pharmacokinetic

studies. Each mouse (average weight, 25 g) received an intravenous bolus via the tail vein of 185 kBq of the radio-RP-HPLC peak purified ^{111}In -radioconjugate in 100 μL of saline. The mice were sacrificed and their tissues and organs excised at 0.25, 1, 4 and 24 hr time points post-injection. The excised tissues were weighed, the ^{111}In activity in each tissue was measured, and the %ID and %ID/g was determined for each tissue. Whole blood %ID and %ID/g was determined under the assumption that the weight of the blood accounted for 6.5% of the body weight of the mouse.

Small Animal SPECT/CT Imaging Studies

The Micro-SPECT/CT is a combined modality unit (microCAT II, Siemens Medical Solutions) equipped with dual pixelated SPECT detectors each coupled to a square 3×3 array of position sensitive photomultiplier tubes. The CT component consists of a CCD x-ray detector and an 80 kVp micro-focus x-ray source (40 μm focal spot). The mice were administered 27.8 – 55.5 MBq of the desired BB2r-targeted peptide in 150 - 200 μL of saline via tail vein injection. At 24 hours post injection, the mice were sacrificed and Micro-SPECT/CT imaging was performed. Micro-SPECT data was collected using a symmetrical 20% photopeak discriminating window and employing a 360° rotation, 60 step acquisition with a 2 mm pinhole collimator. Pinhole tomographic reconstruction of the generated Micro-SPECT data was performed using a 3D-OSEM algorithm with software corrections applied for pinhole misalignments. Micro-CT data acquisition proceeded immediately prior to Micro-SPECT data acquisition. Concurrent image reconstruction was achieved using a Fanbeam (Feldkamp) Filtered back projection algorithm. Micro-SPECT data was fused with anatomical data from Micro-CT in order to accurately determine spatial location of radionuclide uptake within the three dimensional volume. Whole body and axial images were normalized to the highest intensity pixel for each image.

Statistical Analysis

A Student's t-test was utilized to determine statistical significance. A confidence level of 95% was employed in the statistical analysis of this data and $P \leq 0.05$ was considered statistically significant.

Results

Conjugate Synthesis and Radiolabeling

The conjugates were synthesized using standard solid phase peptide synthesis techniques. Typical yields for the 8-AOC, 5-AOS, 8-ADS and Gly-AM2BA peptide conjugates ranged from 47 – 76% as determined by RP-HPLC. Relatively poor yields (12 - 21%) were obtained from the AMBA and Gly-AMBA conjugates. Analysis of the crude product for the AMBA and Gly-AMBA conjugates by RP-HPLC and mass spectrometry revealed that a significant portion of the growing peptides had prematurely terminated. In the syntheses of both the AMBA and Gly-AMBA peptides, ~45% of the crude material was attributed to the AMBA-Gln-Trp-Ala-Val-Gly-His-Leu-Met-NH₂ peptide ($[\text{M}+\text{H}]^+_{\text{calc}} = 1059.5$; $[\text{M}+\text{H}]^+_{\text{obs}} = 1059.5$). Attempts to increase the overall yield of the AMBA and Gly-AMBA conjugates by extending the coupling time and increasing the amount of the amino acids used per coupling cycle were unsuccessful. Mass spectrometric characterization of all conjugates is provided in Table 1.

Labeling and purification of the conjugates with $^{\text{nat}}\text{In}$ and ^{111}In were carried out under similar conditions. Retention times for all conjugates and $^{\text{nat}}/^{111}\text{In}$ -conjugates are given in Table 1. The retention times of the unlabeled conjugates and the $^{\text{nat}}/^{111}\text{In}$ -conjugates were similar (< 1 min separation) and therefore were difficult to resolve due to peak overlap. Addition of excess $^{\text{nat}}\text{CuSO}_4\cdot 5\text{H}_2\text{O}$ to the reaction vial after incubation of the peptide with $^{\text{nat}}/^{111}\text{In}$ resulted in complexation of the $^{\text{nat}}\text{Cu}$ with any available unlabeled conjugate. The $^{\text{nat}}\text{Cu}$ -conjugates

typically had retention times that were ~ 2 min longer relative to the $^{nat/111}\text{In}$ labeled conjugate. This allowed the $^{nat/111}\text{In}$ -conjugate to be easily isolated without concern of collection overlap with the unlabeled conjugate.

In Vitro Cell Binding and Internalization Studies

The BB2r binding affinity of the conjugates and ^{nat}In -conjugates was investigated using in vitro PC-3 cell binding studies (Table 1). The scrambled peptide ^{111}In -DOTA-8-AOC-NONSENSE underwent in vitro and in vivo studies to assist in contrasting specific vs. non-specific binding. With the exception of the scrambled peptide, all of the conjugates and ^{nat}In -conjugates demonstrated nanomolar binding affinities with minimal (< 10%) nonspecific binding. The ^{nat}In -labeled conjugates had IC_{50} values of 0.51 ± 0.05 , 0.7 ± 0.1 , 1.13 ± 0.07 , 1.88 ± 0.06 , 3.2 ± 0.3 and 6.2 ± 0.3 nM for the 8-AOC, Gly-AM2BA, AMBA, Gly-AMBA, 8-ADS and 5-AOS, respectively. In general, the ^{nat}In -conjugates containing aromatic linking groups possessed higher binding affinities for the BB2r than ^{nat}In -conjugates with ether linking groups.

Internalization and efflux of the radioconjugates in PC-3 cells are depicted in Figure 2 and 3, respectively. At 15 min post-incubation, the 8-AOC and Gly-AMBA radioconjugates demonstrated on average the lowest initial percent internalization. The radioconjugates demonstrated little, if any, increase in internalization after the initial 15 minute incubation time point. With the exception of the Gly-AMBA radioconjugate, the radioconjugates demonstrated similar efflux of activity from the PC-3 cells. The Gly-AMBA radioconjugate exhibited an approximate 2 fold increase in efflux of the radioactivity from the cell relative to the other radioconjugates.

Biodistribution Studies

With the exception of the 8-AOC radioconjugate, the in vivo pharmacokinetic properties of the ^{111}In -radioconjugates were initially investigated in normal CF-1 mice. We have previously reported the pharmacokinetic profile of the ^{111}In -DOTA-8-AOC-BBN(7-14) NH_2 radioconjugate in normal CF-1 mice.(9) Results from the in vivo pharmacokinetic studies in normal CF-1 mice at the 1 hr p.i. time point are summarized in Table 2.(26) All of the investigated ^{111}In -radioconjugates demonstrated efficient blood clearance at 1 hr post-injection. Biological clearance of all radioconjugates proceeded primarily through the renal/urinary system with the remaining radioactivity being secreted through the hepatobiliary pathway. At 1 hr post-injection, the kidney retention of the radioconjugates was significantly higher ($P \leq 0.0003$) for the Gly-AMBA (10.60 ± 1.57 %ID/g) and Gly-AM2BA (5.60 ± 2.12 %ID/g) than the other derivatives ($2.40 \pm 0.40 - 2.51 \pm 0.51$). Interestingly, though, the Gly-AMBA and Gly-AM2BA radioconjugates demonstrated the highest clearance of kidney associated activity over time with 0.70 ± 0.08 and 0.67 ± 0.08 , respectively, at the 24 hr p.i. time point. Even though the 5-AOS, 8-ADS and AMBA radioconjugates had significantly less kidney associated activity at 1 hr post-injection, these radioconjugates did not clear as well with 1.29 ± 0.20 , 1.30 ± 0.32 and 1.19 ± 0.18 , respectively, remaining associated with the kidneys at 24 hr post-injection. The rodent pancreas is known to express high densities of the BB2r and therefore provides a convenient in vivo target in which to gauge the efficacy of our radioconjugates.(27) The pancreatic uptake of radioconjugates containing aromatic linking groups was found to be significantly higher ($P \leq 0.0002$) than the radioconjugates with ether linker moieties. The Gly-AMBA radioconjugate demonstrated significantly higher pancreatic uptake (63.35 ± 5.91) than any other radioconjugate studied in CF-1 mice ($P \leq 0.0001$). As expected, the scrambled peptide demonstrated no BB2r specific binding and cleared effectively from the mice with 94.13 ± 0.45 %ID being excreted at 1 hr post-injection. The clearance of the ^{111}In -radioconjugates through the G.I. tract was not surprisingly found to be dependent upon the linker functional group of the radioconjugate. Radioconjugates containing aromatic

linking groups had the highest intestinal uptake at 1 hr post-injection ($P \leq 0.003$). Due to the relatively low in vivo BB2r targeting properties of the ^{111}In -DOTA-5-AOS-BBN(7-14) NH_2 radioconjugate, further investigation of this radioconjugate in the PC-3 tumor mouse model was not performed.

The pharmacokinetic profiles of the 8-AOC, 8-ADS, AMBA, Gly-AMBA and Gly-AM2BA radioconjugates were examined in the SCID mouse model bearing PC-3 tumor xenografts. In vivo non-specific interactions were investigated in the PC-3 tumor bearing mouse model by performing biodistribution studies using the scrambled peptide at 1 hr post-injection. The 1, 4 and 24 hr time points from these studies are summarized in Table 3.(26) At 15 min post-injection, tumor uptake was found to be 6.66 ± 2.00 , 6.21 ± 1.57 , 6.36 ± 1.60 , 4.46 ± 0.81 and 7.76 ± 1.19 %ID/g for the 8-AOC, 8-ADS, AMBA, Gly-AMBA and Gly-AM2BA radioconjugates, respectively. At 24 hr post-injection, 11.4, 19.8, 26.6, 25.8 and 25.5% of the initial uptake was retained in the tumor tissue corresponding respectively to the 8-AOC, 8-ADS, AMBA, Gly-AMBA and Gly-AM2BA radioconjugates. At 1 hr post-injection, the tumor uptake of the targeted radioconjugates was a factor of 3.4 – 5.8 greater than the non-specific binding of the scrambled radioconjugate (0.58 ± 0.20 %ID/g). All of the radioconjugates investigated cleared efficiently from the blood. Clearance of the radioconjugates proceeded largely through the renal/urinary system. Kidney retention was found to be dependent upon the radioconjugate used. The Gly-AMBA and 8-ADS radioconjugates had the largest kidney retention values with 3.71 ± 2.37 and 2.36 ± 0.66 %ID/g, respectively, at 24 hr post-injection. The hepatobiliary retention at 24 hr p.i. ranged from 8 – 15 %ID depending on the radioconjugate. The most striking difference in G.I. tract retention was observed with the aromatic containing radioconjugates having 2 – 4 fold more radioactivity than the 8-AOC and 8-ADS radioconjugates.

Small Animal SPECT/CT Imaging Studies

Micro-SPECT/CT studies were performed in SCID mice bearing bilateral flank PC-3 tumors using the ^{111}In -DOTA-8-AOC-BBN(7-14) NH_2 , ^{111}In -DOTA-AMBA-BBN(7-14) NH_2 , ^{111}In -DOTA-Gly-AMBA-BBN(7-14) NH_2 and ^{111}In -DOTA-Gly-AM2BA-BBN(7-14) NH_2 radioconjugates. The whole body images and the respective axial slices of the PC-3 tumors are depicted in Figure 4 and were acquired at 24 hr post-injection of the radioconjugates. In the fused Micro-SPECT/CT images, visual inspection of the normalized whole body images indicates a substantially smaller tumor to background ratio for the AMBA radioconjugate relative to the 8-AOC, Gly-AMBA and Gly-AM2BA images. However, axial slices of the PC-3 tumor for all the radioconjugates investigated demonstrated substantial accumulation of radioactivity in the tumor tissue with excellent tumor to background ratios. For the AMBA and Gly-AMBA radioconjugates, significant abdominal accumulation is observed likely, as established in the pharmacokinetic studies, due to the retention of radioactivity in the G.I. tract and pancreas. The majority of the non-target retention for the 8-AOC and Gly-AM2BA radioconjugates was located predominantly in the kidneys.

Discussion

The conjugates were synthesized in moderate yields with the exception of the AMBA (yield: 21% by RP-HPLC) and Gly-AMBA (yield: 12% by RP-HPLC) conjugates. Analysis of the AMBA and Gly-AMBA conjugates by RP-HPLC and mass spectrometry revealed that the majority of the crude material prematurely terminated. The major source of peptide termination was found to occur after the *p*-aminobenzoic acid was coupled to the growing peptide during peptide synthesis. The early termination of the peptide is likely attributed to the significantly reduced nucleophilicity of the primary amine of the *p*-aminobenzoic acid due to the lone pair of the 1° amine being tied up in resonance with the aromatic ring. Whereas, the linking group

of the Gly-AM2BA conjugate employs *p*-aminomethylbenzoic acid in which the capability of *p*-orbital conjugation between the amine and the aromatic ring is eliminated by the presence of the benzylmethyl group. Yields for the Gly-AM2BA (yield: 47% by RP-HPLC) conjugate were significantly higher than either the AMBA or Gly-AMBA conjugates.

In our experiments, the addition of $\text{natCu(II)SO}_4 \cdot 5\text{H}_2\text{O}$ to the reaction mixture after the radioconjugates were labeled significantly aided in the separation of the ^{111}In labeled radioconjugate from the unlabeled conjugate. Biological evaluation of the radioconjugate containing a significant amount of unlabeled BBN conjugate in solution would result in significantly reduced uptake of the ^{111}In -BBN analog in BB2r-expressing tissues due to the blocking of available BB2rs by the unlabeled BBN analog. However, Lantry and co-workers recently reported that predose administration of a small amount ($83.2 \mu\text{g}/\text{m}^2$) of a BB2r agonist prior to administration of a radiolabeled BB2r agonist (^{177}Lu -DOTA-Gly-AMBA-BBN(7-14) NH_2) reduced the uptake in the BB2r-rich mouse pancreas, while maintaining the same tumor uptake and retention as studies with no predose.(23) This study suggests that there may be a beneficial effect of having a minimal concentration of unlabeled BB2r-targeting bombesin analogs in administered doses. Further studies are required to determine if such an optimum window of concentration for non-labeled BB2r specific peptides exists.

In vitro competitive BB2r binding assays of the natIn -BBN analogs and unlabeled BBN analogs were performed using [^{125}I -Tyr 4]BBN in PC-3 cells. All natIn -BBN conjugates demonstrated nanomolar binding affinity for the BB2r. The binding affinities followed the trend: alkyl linker > aromatic linkers > ether linkers. All radioconjugates exhibited receptor-mediated internalization and retention of the radioactivity.

In vivo biodistribution studies for each radioconjugate with exception of the 8-AOC radioconjugate were performed using healthy CF-1 mice. Of the five radioconjugates investigated, the radioconjugates containing aromatic linking groups had significantly higher pancreatic retention at 1 hr post-injection ($P \leq 0.0002$). Impressively, the pancreatic retention of the Gly-AMBA radioconjugate ($63.35 \pm 5.91 \text{ \%ID/g}$) was nearly twice that of any of the other radioconjugates investigated. The rationale for the increased in vivo BB2r uptake of Gly-AMBA over the structurally very similar analog Gly-AM2BA is unclear. Kidney retention is an important factor when considering the development of therapeutic radiopharmaceuticals due to potential nephrotoxicity.(28) Even though the Gly-AMBA and Gly-AM2BA radioconjugates initially demonstrated significantly higher kidney retention at 1 hr p.i. compared to the 5-AOS, 8-ADS and AMBA radioconjugates, all of the radioconjugates investigated demonstrated efficient clearance from the kidneys by 24 hr post-injection. The hepatobiliary clearance of the radioconjugates containing ether derived linking groups was significantly greater than radioconjugates containing aromatic linking groups ($P \leq 0.0003$). For diagnostic radiopharmaceuticals, obtaining a good target to non-target ratio is crucial for the generation of easily interpretable clinical diagnostic images. The increased hepatobiliary retention of the radioconjugates with aromatic derivatives is clearly detrimental to obtaining high target to non-target ratios with minimal abdominal background.

Taking the results from the CF-1 pharmacokinetic studies into account, the 8-AOC, 8-ADS, AMBA, Gly-AMBA and Gly-AM2BA radioconjugates were further investigated in a PC-3 tumor bearing mouse model. All of the radioconjugates cleared well from the blood, but the blood associated activities were on average higher for the SCID mice compared to the CF-1 mice at 1 hr post-injection. Like the CF-1 mice, the primary route of clearance of ^{111}In radioactivity from the SCID mice was the renal system. Renal retention of the radioconjugates at 1 hr post-injection was higher in the SCID mouse model relative to what was observed with CF-1 mice. However, the overall trend in renal retention among the radioconjugates was largely unchanged. At 1 hr post-injection, tumor retention followed the trend 8-AOC < 8-ADS < Gly-

AM2BA < Gly-AMBA < AMBA. The AMBA radioconjugate had the highest accumulation in the tumors at the 1 hr time point and was significantly greater than 8-AOC, 8-ADS and Gly-AM2BA ($P = 0.0029, 0.0251, \text{ and } 0.0386$, respectively). No statistically significant differences in tumor uptake were observed using the AMBA and Gly-AM2BA radioconjugates. The radioconjugates containing aromatic groups clearly demonstrate significantly higher retention ($P \leq 0.0213$) in the PC-3 tumor tissue at the 4 hr post-injection time point when compared to the radioconjugates containing hydrocarbon or ether linking moieties. At 24 hr post-injection, the trend in tumor retention was 8-AOC < Gly-AMBA < 8-ADS < AMBA < Gly-AM2BA. Statistical differences among individual radioconjugates were found, but no statistical significance was found in relating the retention of the radioconjugates in the PC-3 tumors to the linking group functionality. Comparison of the ^{111}In -labeled 8-AOC and Gly-AMBA radioconjugates with identical ^{177}Lu -labeled analogs reported by our laboratory and Lantry and co-workers revealed interesting trends in tumor retention with respect to the radionuclide employed.(23,29) The ^{177}Lu -labeled 8-AOC and Gly-AMBA radioconjugates demonstrated tumor retention values at each time point that were $\sim 1.7 - 2.8$ times greater relative to the ^{111}In -labeled 8-AOC and Gly-AMBA radioconjugates suggesting that the choice of radionuclide can have a substantial impact on tumor retention. The pancreatic uptake of the ^{111}In -labeled radioconjugates was consistent in both the CF-1 and SCID mouse models. However, it is noteworthy that the *in vivo* pancreatic uptake of the radioconjugates in both mouse models did not correlate strongly with the *in vivo* tumor uptake of the radioconjugates. The differences in pancreatic and tumor retention could possibly be accounted for by factors such as differences in the tumor vascular systems and/or differences between murine (pancreas) and human (PC-3 tumor) BB2r homology. From these studies, it appears that the methodology that employs normal mouse models (e.g. CF-1) as the sole screening tool for potential BB2r targeting radiopharmaceuticals may be inadequate in predicting the *in vivo* uptake in BB2r positive human tumors.

Micro-SPECT/CT imaging studies of the 8-AOC, AMBA Gly-AMBA and Gly-AM2BA radioconjugates predominantly correlated well with the respective biodistribution studies. Visual inspection of the whole body images clearly illustrates superior tumor visualization with the Gly-AMBA and Gly-AM2BA radioconjugates. Examination of the normalized images also indicated significant abdominal accumulation for AMBA and Gly-AMBA radioconjugates, whereas the 8-AOC and Gly-AM2BA exhibited primarily renal retention as the major source of non-target retention. Comparison of the 8-AOC and Gly-AM2BA radioconjugates reveal considerably higher tumor to kidney ratios for the Gly-AM2BA. The higher tumor to kidney ratios could be potentially significant if a radiotherapeutic derivative of the Gly-AM2BA radioconjugate were investigated. For the 8-AOC and Gly-AM2BA radioconjugates, the whole body images deviate somewhat from the corresponding biodistribution studies in which the retention of activity in both the G.I. tract and pancreas are an order of magnitude greater than the kidneys at the analogous time point. One possible explanation for the deviations between the biodistribution studies and the imaging data could be due to the fact that the preclinical SPECT/CT studies required the ^{111}In -radioconjugates to be administered in a quantity that was approximately three orders of magnitude greater than the biodistribution studies. The disparity in the quantity of the ^{111}In -radioconjugate employed in the studies may affect the pharmacokinetics of the radioconjugates *in vivo*.

In conclusion, we have systematically evaluated the pharmacokinetic profile of several diverse linking groups based upon hydrocarbon, ether and aromatic moieties using *in vitro* studies and *in vivo* pharmacokinetic and SPECT/CT imaging studies. Our studies indicate that radioconjugates incorporating aromatic linking groups, of the type investigated, generally demonstrate significantly higher hepatobiliary retention when compared with either the hydrocarbon or ether linking groups. However, we found that radioconjugates containing aromatic linking groups typically exhibited higher *in vivo* uptake and retention in the murine

pancreas, a BB2r rich tissue, than radioconjugates composed of ether linking groups. Similarly, in BB2r positive human PC-3 tumors, the radioconjugates incorporating aromatic linking groups on average generally demonstrated higher PC-3 tumor retention. The role of linking groups in small peptide receptor-targeted radiopharmaceutical design has largely been viewed as merely a convenient way to adjust the blood retention and overall clearance of the radiopharmaceutical without making substantial alterations to the targeting vector. This study clearly demonstrates the significance of the linking group upon not only the in vivo clearance of the radiopharmaceutical, but on the in vivo uptake and retention of the BB2r-targeted agent in tumor tissue. The design of future BB2r-targeted agents should include a careful consideration of the effect linking group functionality has upon tumor targeting and retention. Further more, in evaluating the uptake and retention of the radioconjugates in mouse and human BB2r expressing tissues, we find that the uptake and retention of the radioconjugates in human PC-3 tumors did not correlate strongly with the pharmacokinetic profiles obtained from the murine pancreas. This indicates that relying solely on BB2r expression in the murine pancreas to optimize or screen BB2r-targeted agents for human BB2r expressing tumors may not be appropriate. Future work will focus on evaluating and optimizing the pharmacokinetic profile of cleavable linking groups and linking groups composed of other non-standard amino acids using the BBN paradigm.

Supplementary Material

Refer to Web version on PubMed Central for supplementary material.

Acknowledgements

The authors gratefully acknowledge the support of postdoctoral fellowship (PFTED-07-267-01-SIED) (JCG) awarded by the Canary Foundation and the American Cancer Society and additional funding from the National Cancer Institute DHHS-R01-CA72942 (TJH), DHHS-1P50-CA13013 (WAV), and the American Cancer Society RSG-99-331-04-CDD (TJH). The authors would further like to acknowledge Dr. Nathan D. Leigh and the Mass Spectrometry Facility in the Department of Chemistry at the University of Missouri-Columbia for the collection and assistance in interpretation of the mass spectra in this manuscript. This work was supported with the resources and the use of facilities at the Harry S Truman Memorial VA Hospital.

References

1. Smith CJ, Volkert WA, Hoffman TJ. Radiolabeled peptide conjugates for targeting of the bombesin receptor superfamily subtypes. *Nucl Med Biol* 2005;32:733–740. [PubMed: 16243649]
2. Smith CJ, Volkert WA, Hoffman TJ. Gastrin releasing peptide (GRP) receptor targeted radiopharmaceuticals: A concise update. *Nucl Med Biol* 2003;30:861–868. [PubMed: 14698790]
3. Cornelio DB, Roesler R, Schwartzmann G. Gastrin-releasing peptide receptor as a molecular target in experimental anticancer therapy. *Ann Oncol* 2007;18:1457–1466. [PubMed: 17351255]
4. Reubi JC, Wenger S, Schmuckli-Maurer J, Schaer J-C, Gugger M. Bombesin receptor subtypes in human cancers: Detection with the universal radioligand ^{125}I -[D-TYR⁶, β -ALA¹¹, PHE¹³, NLE¹⁴] bombesin(6-14). *Clin Cancer Res* 2002;8:1139–1146. [PubMed: 11948125]
5. Gugger M, Reubi JC. Gastrin-releasing peptide receptors in non-neoplastic and neoplastic human breast. *Am J Pathol* 1999;155:2067–2076. [PubMed: 10595936]
6. Markwalder R, Reubi JC. Gastrin-releasing peptide receptors in the human prostate: Relation to neoplastic transformation. *Cancer Res* 1999;59:1152–1159. [PubMed: 10070977]
7. Jensen RT, Battey JF, Spindel ER, Benya RV. International union of pharmacology. LXVIII. Mammalian bombesin receptors: Nomenclature, distribution, pharmacology, signaling, and functions in normal and disease states. *Pharmacol Rev* 2008;60:1–42. [PubMed: 18055507]
8. Garrison JC, Rold TL, Sieckman GL, Figueroa SD, Volkert WA, Jurisson SS, Hoffman TJ. In vivo evaluation and small-animal PET/CT of a prostate cancer mouse model using ^{64}Cu bombesin analogs: Side-by-side comparison of the CB-TE2A and DOTA chelation systems. *J Nucl Med* 2007;48:1327–1337. [PubMed: 17631556]

9. Hoffman TJ, Gali H, Smith CJ, Sieckman GL, Hayes DL, Owen NK, Volkert WA. Novel series of ^{111}In -labeled bombesin analogs as potential radiopharmaceuticals for specific targeting of gastrin-releasing peptide receptors expressed on human prostate cancer cells. *J Nucl Med* 2003;44:823–831. [PubMed: 12732685]
10. Smith CJ, Gali H, Sieckman GL, Hayes DL, Owen NK, Mazuru DG, Volkert WA, Hoffman TJ. Radiochemical investigations of ^{177}Lu -DOTA-8-Aoc-BBN[7-14] NH_2 : An in vitro/in vivo assessment of the targeting ability of this new radiopharmaceutical for PC-3 human prostate cancer cells. *Nucl Med Biol* 2003;30:101–109. [PubMed: 12623108]
11. Smith CJ, Gali H, Sieckman GL, Higginbotham C, Volkert WA, Hoffman TJ. Radiochemical investigations of $^{99\text{m}}\text{Tc}$ - $\text{N}_3\text{S-X-BBN}$ [7-14] NH_2 : An in vitro/in vivo structure-activity relationship study where X = 0-, 3-, 5-, 8-, and 11-carbon tethering moieties. *Bioconjugate Chem* 2003;14:93–102.
12. Moustapha ME, Ehrhardt GJ, Smith CJ, Szajek LP, Eckelman WC, Jurisson SS. Preparation of cyclotron-produced ^{186}Re and comparison with reactor-produced ^{186}Re and generator-produced ^{188}Re for the labeling of bombesin. *Nucl Med Biol* 2006;33:81–89. [PubMed: 16459262]
13. Hu F, Cutler CS, Hoffman T, Sieckman G, Volkert WA, Jurisson SS. Pm-149 DOTA bombesin analogs for potential radiotherapy - In vivo comparison with Sm-153 and Lu-177 labeled DO3A-amide- $\beta\text{Ala-BBN}$ (7-14) NH_2 . *Nucl Med Biol* 2002;29:423–430. [PubMed: 12031877]
14. Zhang HW, Schuhmacher J, Waser B, Wild D, Eisenhut M, Reubi JC, Maecke HR. DOTA-PESIN, a DOTA-conjugated bombesin derivative designed for the imaging and targeted radionuclide treatment of bombesin receptor-positive tumours. *Eur J Nucl Med Mol I* 2007;34:1198–1208.
15. Zhang X, Cai W, Cao F, Schreiber E, Wu Y, Wu JC, Xing L, Chen X. ^{18}F -labeled bombesin analogs for targeting GRP receptor-expressing prostate cancer. *J Nucl Med* 2006;47:492–501. [PubMed: 16513619]
16. Zhang H, Chen J, Waldherr C, Hinni K, Waser B, Reubi JC, Maecke HR. Synthesis and evaluation of bombesin derivatives on the basis of pan-bombesin peptides labeled with indium-111, lutetium-177, and yttrium-90 for targeting bombesin receptor-expressing tumors. *Cancer Res* 2004;64:6707–6715. [PubMed: 15374988]
17. Volkert WA, Hoffman TJ. Therapeutic radiopharmaceuticals. *Chem Rev* 1999;99:2269–2292. [PubMed: 11749482]
18. Prasanphanich AF, Nanda PK, Rold TL, Ma LX, Lewis MR, Garrison JC, Hoffman TJ, Sieckman GL, Figueroa SD, Smith CJ. [^{64}Cu -NOTA-8-Aoc-BBN(7-14) NH_2] targeting vector for positron-emission tomography imaging of gastrin-releasing peptide receptor-expressing tissues. *Proc Natl Acad Sci U S A* 2007;104:12462–12467. [PubMed: 17626788]
19. Liu S, Edwards DS. Bifunctional chelators for therapeutic lanthanide radiopharmaceuticals. *Bioconjugate Chem* 2001;12:7–34.
20. Anderson CJ, Welch MJ. Radiometal labeled agents (non-technetium) for diagnostic imaging. *Chem Rev* 1999;99:2219–2234. [PubMed: 11749480]
21. Trail PA, King HD, Dubowchik GM. Monoclonal antibody drug immunoconjugates for targeted treatment of cancer. *Cancer Immunol Immun* 2003;52:328–337.
22. Smith-Jones PM, Stolz B, Albert R, Knecht H, Bruns C. Synthesis, biodistribution and renal handling of various chelate-somatostatin conjugates with metabolizable linking groups. *Nucl Med Biol* 1997;24:761–769. [PubMed: 9428603]
23. Lantry LE, Cappelletti E, Maddalena ME, Fox JS, Feng W, Chen J, Thomas R, Eaton SM, Bogdan NJ, Arunachalam T, Reubi JC, Raju N, Metcalfe EC, Lattuada L, Linder KE, Swenson RE, Tweedle MF, Nunn AD. ^{177}Lu -AMBA: synthesis and characterization of a selective ^{177}Lu -labeled GRP-R agonist for systemic radiotherapy of prostate cancer. *J Nucl Med* 2006;47:1144–52. [PubMed: 16818949]
24. Maina T, Nock BA, Zhang H, Nikolopoulou A, Waser B, Reubi J-C, Maecke HR. Species differences of bombesin analog interactions with GRP-R define the choice of animal models in the development of GRP-R-targeting drugs. *J Nucl Med* 2005;46:823–830. [PubMed: 15872357]
25. Prasanphanich AF, Lane SR, Figueroa SD, Ma LX, Rold TL, Sieckman GL, Hoffman TJ, McCrate JM, Smith CJ. The effects of linking substituents on the in vivo behavior of site-directed, peptide-based, diagnostic radiopharmaceuticals. *In Vivo* 2007;21:1–16. [PubMed: 17354608]

26. Please see the supporting information for a complete listing of the biodistribution time points for the radioconjugates in CF-1 mice (1, 4 and 24 hr) and PC-3 tumor bearing SCID mice (0.25, 1, 4, and 24 hr).
27. Waser B, Eltschinger V, Linder K, Nunn A, Reubi JC. Selective in vitro targeting of GRP and NMB receptors in human tumours with the new bombesin tracer ^{177}Lu -AMBA. *Eur J Nucl Med Mol I* 2007;34:95–100.
28. Lambert B, Cybulla M, Weiner SM, Van De Wiele C, Ham H, Dierckx RA, Otte A. Renal toxicity after radionuclide therapy. *Radiat Res* 2004;161:607–611. [PubMed: 15161361]
29. Johnson CV, Shelton T, Smith CJ, Ma L, Perry MC, Volkert WA, Hoffman TJ. Evaluation of combined Lu-177-DOTA-8-AOC-BBN (7-14)NH₂ GRP receptor-targeted radiotherapy and chemotherapy in PC-3 human prostate tumor cell xenografted SCID mice. *Cancer Biother Radiopharm* 2006;21:155–166. [PubMed: 16706636]

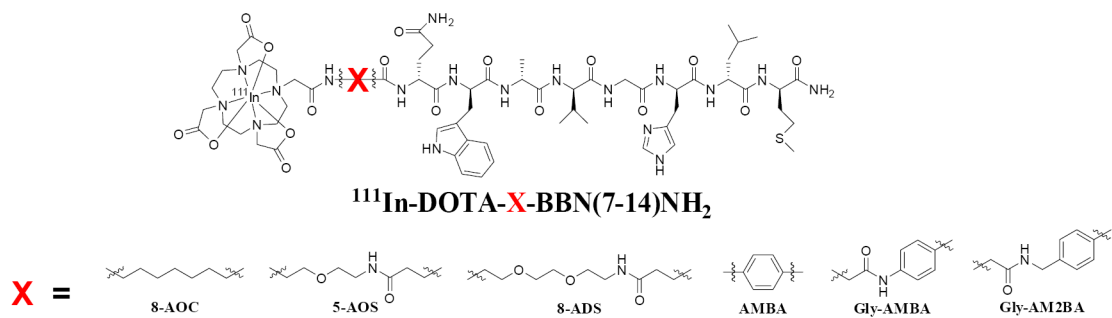


Figure 1.
Structure of ^{111}In -labeled BBN analogs

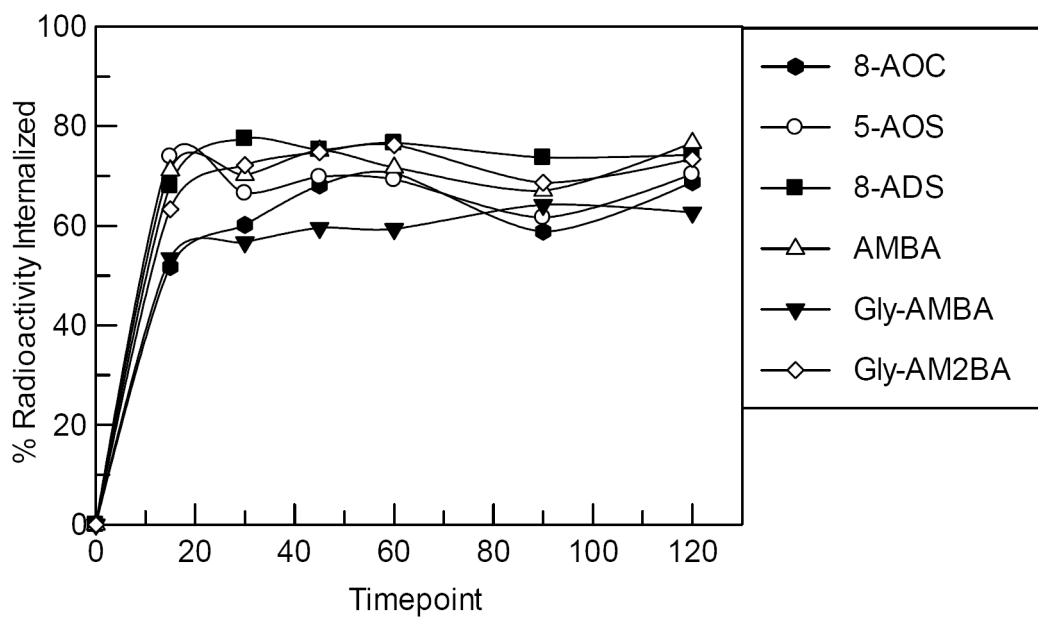


Figure 2. Internalization assays in PC-3 cells using the ^{111}In -BBN radioconjugates ($n = 4$ for each radioconjugate).

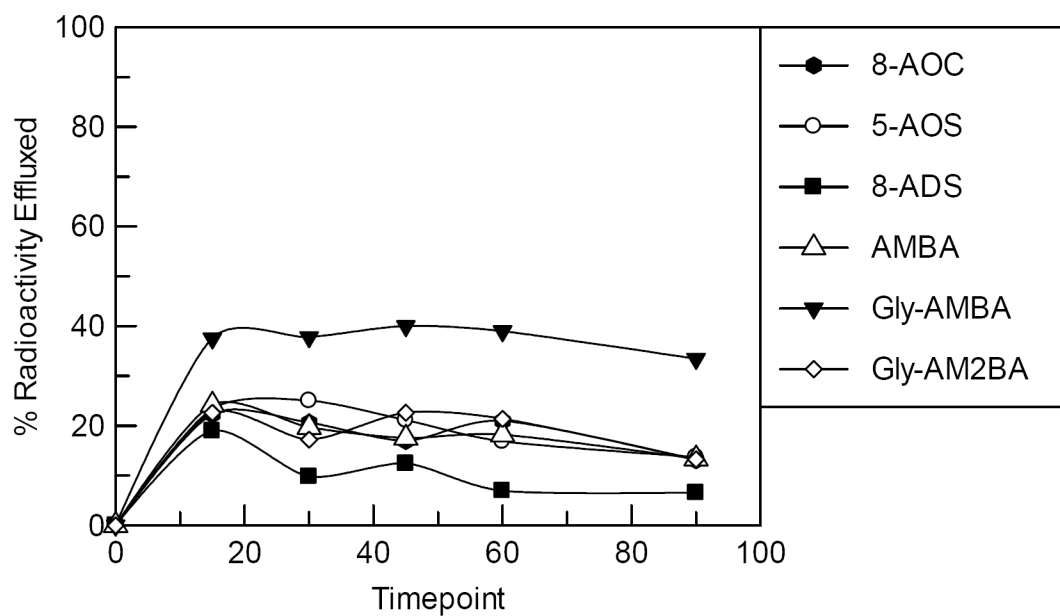


Figure 3. Efflux assays in PC-3 cells using the ^{111}In -BBN radioconjugates (n = 4 for each radioconjugate).

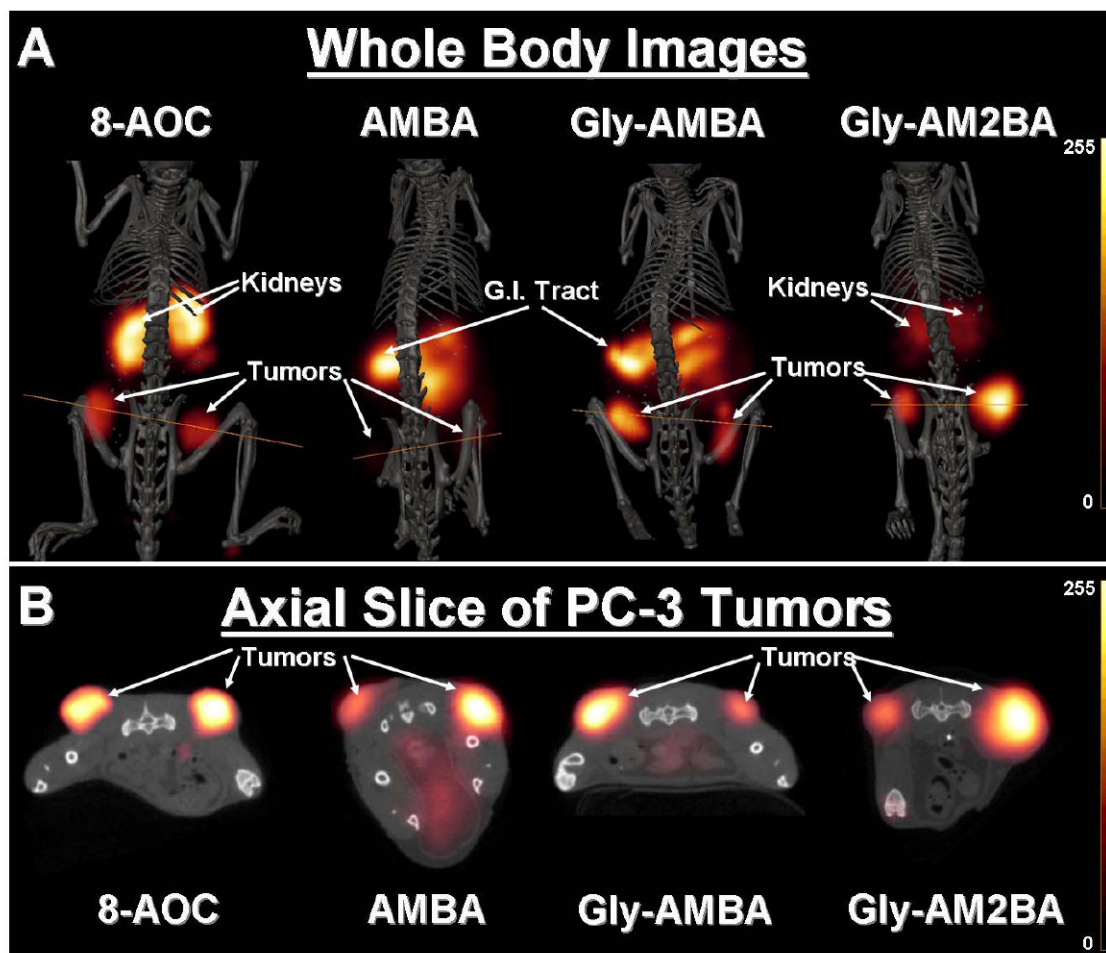


Figure 4.

Small animal SPECT/CT imaging performed 24 hr post-injection in PC-3 tumor bearing SCID mice using ^{111}In -DOTA-8-AOC-BBN(7-14) NH_2 , ^{111}In -DOTA-AMBA-BBN(7-14) NH_2 , ^{111}In -DOTA-Gly-AMBA-BBN(7-14) NH_2 and ^{111}In -DOTA-Gly-AM2BA-BBN(7-14) NH_2 . (A) Whole body images. (B) Axial slices of the PC-3 tumors corresponding to the respective transverse plane depicted in the whole body images. Each whole body and axial image was normalized to the highest intensity pixel for each image.

Table 1
Mass spectrometric values, HPLC retention times and IC₅₀ concentrations for the conjugates investigated.

Analog	Molecular Formula	MS Calculated	MS Observed	RP-HPLC t _r (min) ^b	IC ₅₀ (nM) ^c
DOTA-8-AOC-NONSENSE ^a	C ₆₇ H ₁₀₆ N ₁₈ O ₁₇ S	1467.8	1468.0	16.4	> 10,000
DOTA-8-AOC-BBN(7-14)NH ₂	C ₆₇ H ₁₀₆ N ₁₈ O ₁₇ S	1467.8	1468.0	13.6	-----
DOTA-5-AOS-BBN(7-14)NH ₂	C ₆₇ H ₁₀₅ N ₁₉ O ₁₉ S	1512.8	1512.8	11.3	5.3 ± 0.7
DOTA-8-ADS-BBN(7-14)NH ₂	C ₆₉ H ₁₀₉ N ₁₉ O ₂₀ S	1556.8	1556.8	11.3	11 ± 1
DOTA-AMBA-BBN(7-14)NH ₂	C ₆₆ H ₉₆ N ₁₈ O ₁₇ S	1445.7	1445.7	13.2	3.3 ± 0.5
DOTA-Gly-AMBA-BBN(7-14)NH ₂	C ₆₈ H ₉₉ N ₁₉ O ₁₈ S	1502.7	1502.7	12.5	2.4 ± 0.2
DOTA-AM2BA-BBN(7-14)NH ₂	C ₆₉ H ₁₀₁ N ₁₉ O ₁₈ S	1516.7	1516.5	13.2	1.4 ± 0.2
In-DOTA-8-AOC-NONSENSE ^a	C ₆₇ H ₁₀₃ N ₁₈ O ₁₇ Sn	1579.6	1579.9	17.0	> 10,000
In-DOTA-8-AOC-BBN(7-14)NH ₂	C ₆₇ H ₁₀₃ N ₁₈ O ₁₇ Sn	1579.6	1579.7	13.5	0.51 ± 0.05
In-DOTA-5-AOS-BBN(7-14)NH ₂	C ₆₇ H ₁₀₂ N ₁₉ O ₁₉ Sn	1624.6	1624.4	10.8	6.2 ± 0.3
In-DOTA-8-ADS-BBN(7-14)NH ₂	C ₆₉ H ₁₀₆ N ₁₉ O ₂₀ Sn	1668.7	1668.7	11.6	3.2 ± 0.3
In-DOTA-AMBA-BBN(7-14)NH ₂	C ₆₆ H ₉₃ N ₁₈ O ₁₇ Sn	1557.6	1557.6	12.6	1.13 ± 0.07
In-DOTA-Gly-AMBA-BBN(7-14)NH ₂	C ₆₈ H ₉₆ N ₁₉ O ₁₈ Sn	1614.6	1614.4	12.2	1.88 ± 0.06
In-DOTA-Gly-AM2BA-BBN(7-14)NH ₂	C ₆₉ H ₉₈ N ₁₉ O ₁₈ Sn	1628.6	1628.8	13.0	0.7 ± 0.1

^aNon-Sense peptide sequence: H-M-G-W-L-A-Q-V-NH₂

^bRP-HPLC methods described in Materials and Methods sections.

^cIn vitro binding assays were performed in triplicate.

Table 2

Biodistribution studies of ^{111}In -DOTA-5-AOS-BBN(7-14) NH_2 , ^{111}In -DOTA-8-ADS-BBN(7-14) NH_2 , ^{111}In -DOTA-AMBA-BBN(7-14) NH_2 , ^{111}In -DOTA-Gly-AM2BA-BBN(7-14) NH_2 , and ^{111}In -DOTA-AMBA-BBN(7-14) NH_2 , ^{111}In -DOTA-Gly-AM2BA-BBN(7-14) NH_2 and ^{111}In -DOTA-8-AOC-NONSENSE at 1 hr post-injection in CF-1 mice.

Tissue	5-AOS	8-ADS	AMBA	Gly-AMBA	Gly-AM2BA	Nonsense
Blood	0.16 ± 0.06	0.10 ± 0.01	0.16 ± 0.03	0.19 ± 0.04	0.10 ± 0.03	0.23 ± 0.02
Heart	0.04 ± 0.06	0.07 ± 0.02	0.10 ± 0.02	0.18 ± 0.04	0.08 ± 0.02	0.13 ± 0.02
Lung	0.24 ± 0.07	0.21 ± 0.09	0.25 ± 0.07	0.57 ± 0.25	0.32 ± 0.11	0.23 ± 0.03
Liver	0.16 ± 0.01	0.10 ± 0.01	0.14 ± 0.03	0.19 ± 0.02	0.14 ± 0.01	0.42 ± 0.03
Stomach	0.68 ± 0.16	0.44 ± 0.09	0.74 ± 0.11	2.27 ± 0.52	0.92 ± 0.17	0.27 ± 0.21
Small Intestines (%ID)	4.90 ± 0.33	7.44 ± 0.98	12.49 ± 1.21	10.33 ± 1.36	8.93 ± 1.18	1.04 ± 0.29
Large Intestines (%ID)	1.79 ± 0.29	2.34 ± 0.50	4.57 ± 1.19	6.18 ± 0.44	4.00 ± 0.44	0.19 ± 0.08
Kidney	2.44 ± 0.34	2.51 ± 0.51	2.40 ± 0.40	10.60 ± 1.57	5.60 ± 2.12	1.92 ± 0.60
Spleen	0.86 ± 0.17	0.96 ± 0.33	1.50 ± 0.19	2.90 ± 0.54	1.99 ± 0.78	0.14 ± 0.02
Brain	0.02 ± 0.02	0.01 ± 0.01	0.02 ± 0.00	0.04 ± 0.01	0.02 ± 0.01	0.02 ± 0.00
Pancreas	14.04 ± 2.24	18.85 ± 2.25	28.85 ± 2.73	63.35 ± 5.91	36.58 ± 5.27	0.09 ± 0.03
Muscle	0.07 ± 0.02	0.05 ± 0.01	0.07 ± 0.01	0.13 ± 0.02	0.06 ± 0.02	0.05 ± 0.01
Bone	0.28 ± 0.09	0.14 ± 0.04	0.18 ± 0.07	0.83 ± 0.04	0.34 ± 0.07	0.09 ± 0.04
Excretion (%ID) ^a	83.57 ± 2.83	82.24 ± 1.31	68.43 ± 2.15	58.17 ± 2.22	72.27 ± 1.87	94.13 ± 0.45

Organ uptake values expressed as %ID/g and n = 5 unless otherwise noted.

^aExcretion values were calculated using the activity values associated with the excreted urine and bladder contents at the time of sacrifice.

Table 3

Biodistribution studies of ^{111}In -DOTA-8-AOC-BBN(7-14) NH_2 , ^{111}In -DOTA-8-ADS-BBN(7-14) NH_2 , ^{111}In -DOTA-8-AMBA-BBN(7-14) NH_2 , ^{111}In -DOTA-AMBA-BBN(7-14) NH_2 and ^{111}In -DOTA-Gly-AM2BA-BBN(7-14) NH_2 at 1, 4 and 24 hr post-injection in PC-3 tumor bearing SCID mice.

Tissue	8-AOC	8-ADS	AMBA	Gly-AMBA	Gly-AM2BA	Nonsense
<i>1 hr p.i.</i>						
Blood	0.24 ± 0.03	0.28 ± 0.17	0.33 ± 0.23	0.64 ± 0.25	0.15 ± 0.07 ^b	0.35 ± 0.08
Heart	0.19 ± 0.20	0.10 ± 0.03	0.26 ± 0.21	0.38 ± 0.11	0.11 ± 0.05 ^b	0.19 ± 0.09
Lung	0.40 ± 0.09	0.36 ± 0.21	0.59 ± 0.40	0.72 ± 0.26	0.39 ± 0.21 ^b	0.44 ± 0.12
Liver	0.54 ± 0.09	0.17 ± 0.03	0.31 ± 0.05	0.40 ± 0.13	0.23 ± 0.11 ^b	0.70 ± 0.08
Stomach	0.89 ± 0.40	0.73 ± 0.26	0.91 ± 0.18	2.25 ± 1.04	1.20 ± 0.33 ^b	0.20 ± 0.18
Small Intestines (%ID)	9.95 ± 0.58	5.59 ± 0.88	6.43 ± 0.98	9.95 ± 1.82	9.52 ± 1.65 ^b	1.04 ± 0.25
Large Intestines (%ID)	1.65 ± 0.14	2.34 ± 0.67	2.29 ± 0.20	5.22 ± 0.49	4.07 ± 0.53 ^b	0.28 ± 0.17
Kidney	4.41 ± 1.16	3.54 ± 0.36	5.69 ± 1.51	17.34 ± 7.45	6.00 ± 3.05 ^b	3.10 ± 0.37
Spleen	0.54 ± 0.25	0.43 ± 0.14	0.90 ± 0.26	1.97 ± 0.63	0.65 ± 0.23 ^b	0.22 ± 0.06
Brain	0.02 ± 0.01	0.02 ± 0.01	0.02 ± 0.01	0.05 ± 0.03	0.03 ± 0.02 ^b	0.03 ± 0.02
Pancreas	30.85 ± 5.07	19.22 ± 1.89	30.15 ± 5.90	46.85 ± 6.13	28.55 ± 1.46 ^b	0.12 ± 0.02
Muscle	0.06 ± 0.01	0.06 ± 0.01	0.09 ± 0.04	0.21 ± 0.05	0.09 ± 0.03 ^b	0.12 ± 0.02
Bone	0.26 ± 0.20	0.12 ± 0.07	0.26 ± 0.11	0.93 ± 0.34	0.63 ± 0.35 ^b	0.22 ± 0.11
Tumor	1.95 ± 1.07	2.53 ± 0.78	3.34 ± 0.70	2.97 ± 0.88	2.68 ± 0.62 ^b	0.58 ± 0.20
Excretion (%ID) ^d	72.54 ± 0.96	80.67 ± 0.74	78.69 ± 2.53	54.64 ± 4.43	67.23 ± 1.02 ^b	90.85 ± 3.78
<i>4 hr p.i.</i>						
Blood	0.03 ± 0.01	0.02 ± 0.01	0.06 ± 0.02	0.19 ± 0.04	0.02 ± 0.01	-----
Heart	0.03 ± 0.02	0.04 ± 0.01	0.06 ± 0.03	0.21 ± 0.16	0.03 ± 0.03	-----
Lung	0.14 ± 0.06	0.13 ± 0.09	0.16 ± 0.08	0.24 ± 0.15	0.11 ± 0.03	-----
Liver	0.15 ± 0.02	0.13 ± 0.03	0.28 ± 0.08	0.25 ± 0.04	0.19 ± 0.08	-----
Stomach	0.44 ± 0.31	0.42 ± 0.11	0.41 ± 0.15	1.09 ± 0.40	0.76 ± 0.21	-----
Small Intestines (%ID)	3.06 ± 1.00	2.01 ± 0.38	4.59 ± 0.88	6.94 ± 1.17	4.04 ± 0.94	-----
Large Intestines (%ID)	8.67 ± 2.96	7.13 ± 1.75	4.05 ± 0.80	5.79 ± 1.27	6.22 ± 1.16	-----
Kidney	2.15 ± 0.32	3.92 ± 0.86	4.28 ± 1.10	7.22 ± 2.67	3.24 ± 1.18	-----
Spleen	0.34 ± 0.09	0.33 ± 0.09	0.60 ± 0.23	1.76 ± 0.91	1.98 ± 2.40	-----

Tissue	8-AOC	8-ADS	AMBA	Gly-AMBA	Gly-AM2BA	Nonsense
Brain	0.01 ± 0.00	0.01 ± 0.00	0.01 ± 0.01	0.04 ± 0.02	0.01 ± 0.01	-----
Pancreas	21.51 ± 3.45	18.04 ± 1.47	30.53 ± 5.35	38.95 ± 6.32	35.12 ± 8.20	-----
Muscle	0.02 ± 0.01	0.03 ± 0.02	0.04 ± 0.02	0.03 ± 0.05	0.04 ± 0.01	-----
Bone	0.12 ± 0.03	0.14 ± 0.02	0.33 ± 0.21	0.65 ± 0.44	0.29 ± 0.10	-----
Tumor	1.10 ± 0.23	1.61 ± 0.57	2.42 ± 0.81	2.46 ± 0.90	2.81 ± 0.56	-----
Excretion (%ID) ^a	78.27 ± 4.22	84.82 ± 2.31	81.42 ± 2.85	68.74 ± 2.35	78.40 ± 2.48	-----
<i>24 hr p.i.</i>						
Blood	0.01 ± 0.00	0.01 ± 0.00	0.02 ± 0.00	0.08 ± 0.04	0.01 ± 0.01	-----
Heart	0.02 ± 0.02	0.02 ± 0.01	0.04 ± 0.01	0.14 ± 0.09	0.02 ± 0.02	-----
Lung	0.07 ± 0.03	0.06 ± 0.01	0.08 ± 0.02	0.15 ± 0.06	0.10 ± 0.04	-----
Liver	0.06 ± 0.01	0.07 ± 0.01	0.21 ± 0.03	0.26 ± 0.09	0.11 ± 0.06	-----
Stomach	0.11 ± 0.04	0.17 ± 0.03	0.20 ± 0.08	1.33 ± 0.39	0.63 ± 0.28	-----
Small Intestines (%ID)	1.30 ± 0.30	1.23 ± 0.23	3.43 ± 0.56	5.33 ± 0.64	2.13 ± 0.34	-----
Large Intestines (%ID)	0.93 ± 0.13	0.86 ± 0.14	1.59 ± 0.11	2.84 ± 0.41	2.69 ± 1.19	-----
Kidney	0.72 ± 0.09	2.36 ± 0.66	1.90 ± 0.47	3.71 ± 2.37	1.40 ± 0.85	-----
Spleen	0.28 ± 0.36	0.33 ± 0.08	0.45 ± 0.09	1.28 ± 0.77	0.97 ± 0.73	-----
Brain	0.00 ± 0.00	0.01 ± 0.00	0.01 ± 0.00	0.04 ± 0.04	0.01 ± 0.00	-----
Pancreas	10.70 ± 2.40	17.04 ± 1.65	23.84 ± 2.97	28.19 ± 4.88	13.39 ± 3.20	-----
Muscle	0.01 ± 0.01	0.02 ± 0.01	0.02 ± 0.01	0.11 ± 0.07	0.02 ± 0.02	-----
Bone	0.12 ± 0.04	0.09 ± 0.02	0.15 ± 0.03	0.75 ± 0.33	0.23 ± 0.13	-----
Tumor	0.76 ± 0.21	1.23 ± 0.30	1.69 ± 0.34	1.15 ± 0.57	1.96 ± 0.72	-----
Excretion (%ID) ^a	93.72 ± 0.65	91.71 ± 0.89	87.35 ± 1.06	78.62 ± 1.88	89.61 ± 1.32	-----

Organ uptake values expressed as %ID/g and n = 5 unless otherwise noted.

^aThe biodistribution study of ¹¹¹In-DOTA-8-AOC-NONSENSE was performed at 1 hr post-injection in PC-3 tumor bearing SCID mice.

^bExcretion values at 1, 4 and 24 hr time points were calculated using the activity values associated with the excreted urine and bladder contents at the time of sacrifice; at the 24 hr time point, excretion values also included the activity associated with fecal material.

^cn = 4